energies

MDPI

Article

Process Optimization of Pellet Manufacturing from Mixed Materials in Ultrasonic Vibration-Assisted Pelleting

Wentao Li [1], Rongwei Yu [1], Lina Luo [2,*] and Hongying Shi [3]

[1] College of Engineering, Heilongjiang Bayi Agricultural University, Daqing 163319, China; yuesetingquan@byau.edu.cn (W.L.)
[2] Department of New Energy Science and Engineering, School of Engineering, Northeast Agricultural University, Harbin 150030, China
[3] Heilongjiang Boneng Ecological Environmental Protection Co., Ltd., Harbin 150028, China
* Correspondence: luolina@neau.edu.cn

Abstract: Achieving carbon neutrality and alleviating the rural energy predicament are crucial aspects in rural areas, particularly in the severe cold regions of northeast China. Pellets serve as clean, renewable energy sources and are ideal alternative fuels. This study investigated the influencing factors and effects of mixed raw materials in ultrasonic vibration-assisted pelleting (UV-A pelleting). Rice straw and corn stover were mixed to produce pellets, and a central composite rotatable design (CCRD) was conducted to analyze the variables and their interactions on pellet density and durability. Mathematical regression models for pellet density and durability were established and then validated through ANOVA analysis. The results showed that all variables significantly affected the density and durability of pellets. The mixing ratio had a greater impact on pellet durability compared to density due to differences in ingredients. The optimal combination of process parameters included a mixing ratio of 25%, molding pressure of 4 MPa, pelleting time of 37 s, and ultrasonic power output at 200 W, resulting in a pellet density of 1301.18 kg/m^3 with a durability reaching 94.26%. The desirability value (0.997) under these optimal conditions confirmed the validity of the models; further experiments also verified their effectiveness. The combustion of the optimized pellet was analyzed using thermogravimetric (TG) and derivative thermogravimetric (DTG) analysis in an air atmosphere. Four combustion stages and ignition temperature were provided.

Keywords: process optimization; ultrasonic vibration-assisted pelleting; mixed materials; pellet properties

Citation: Li, W.; Yu, R.; Luo, L.; Shi, H. Process Optimization of Pellet Manufacturing from Mixed Materials in Ultrasonic Vibration-Assisted Pelleting. *Energies* **2024**, *17*, 2087. https://doi.org/10.3390/en17092087

Academic Editor: Albert Ratner

Received: 7 April 2024
Revised: 18 April 2024
Accepted: 23 April 2024
Published: 26 April 2024

1. Introduction

The efficient utilization of agricultural residues as a high-quality resource is an integral component of China's 2030 carbon peak action plan. The biomass resources in China possess significant storage capacity, a wide range of types, extensive sources, and robust sustainability [1]. According to estimates, the total amount of agricultural residues that can be collected in China is approximately 876 million tons [2]. The theoretical yield of straw in northeast China exceeds 190 million tons per year [3]. One of the traditional treatments of straw is mostly pulverized and returned to the field. Due to the slow degradation rate of straw in cold climates [4], it generally takes 2 years to degrade completely under deeply buried conditions. Returning straw to the field for many years leads to the increasing accumulation of straw in the soil, which is turned over to a shallow soil layer during the preparation of the land, resulting in frequent blockage or seeds being sown into the straw, which greatly reduces the emergence rate. As the northeast is a high-cold region, regional fuel utilization is important, which can not only effectively solve the current energy crisis [5] but also avoid the adverse impact on the environment caused by straw burning in the field and waste on the spot and promote the construction and development of beautiful rural areas [6].

Compared to biochemical conversion and thermochemical conversion, pellets are a more cost-effective biofuel for their uniform shape, convenient storage, transportation, and simple production process [7–9]. Conventional methods employed for pellets production encompass screw extrusion, piston press, and ring die techniques [10–12]. According to the differences in process characteristics, it can be divided into hot-pressing molding and room-temperature molding. The factors affecting pellets can be divided into two aspects. One is the characteristics of the raw materials, mainly including the type, the particle size, and the water content. The other is process parameters, mainly including molding pressure, time, temperature, and binder.

In the traditional method, the heat generated by the resistance wire or friction causes the material to undergo softening and bonding under external force, resulting in the formation of pellets. Wear, tear, and high energy consumption were inevitable in the process. The primary solutions were to reduce raw material particle size and soften lignin by increasing the heating temperature or adding a binder to decrease wear and energy consumption. However, the effect is not ideal. The limitations of traditional molding equipment have greatly hindered the improvement of pellet quality. To address these issues, the concept of ultrasonic vibration-assisted pelleting (UV-A pelleting) was introduced to produce pellets at room temperature without the need for high pressure or additional adhesive [13–15]. This approach significantly reduced wear and energy consumption. Zhang et al. [15] discovered that increasing ultrasonic power resulted in higher density and durability of wheat straw pellets. A predictive model for pellet density using response surface methodology (RSM) was developed specifically for UV-A pelleting of wheat straw [16]. Furthermore, corn stover pellets produced through UV-A pelleting exhibited comparable density and durability to those made by ring-die pelleting [17].

However, previous research primarily focused on single raw materials such as sorghum stalks, wheat stalks, and corn stover. The molding process varied due to differences in cellulose content, lignin content, and other components among different types of raw materials used. Therefore, it remained unclear how mixed raw materials would perform in UV-A pelleting for pellet production. Thus, the primary objective of this study was first to seek the feasibility of mixing corn straw with rice straw for producing pellets using UV-A pelleting technology while analyzing their physical properties. Secondly, optimal conditions were determined to achieve higher pellet density and pellet durability. Lastly, the combustion of the optimized pellet was analyzed using thermogravimetric analysis (TG) and derivative thermogravimetric (DTG).

2. Materials and Methods

2.1. Materials and Experimental Setup

The materials used in this study were corn stover and rice straw obtained from the experimental field of Heilongjiang Bayi Agricultural University. After undergoing natural drying, the raw materials were cut into small sections and then milled into particles less than 2 mm using a high-speed multi-functional crusher (Model YB-1000, Jinhua, China), as shown in Figure 1. Elemental analysis and major chemical components of corn and rice straw are shown in Tables 1 and 2, respectively. The moisture content of the particles was adjusted to 10% with distilled water [18]. The mixing ratio for pellet production was determined based on the quality of rice straw and corn straw.

Table 1. Elemental analysis of corn and rice straw.

Sample	C/%	H/%	O/%	N/%	S/%	Ash/%
Corn Stover	51.43	7.13	37.64	0.79	0.38	7.89
Rice straw	47.36	7.59	39.73	0.86	0.27	6.74

Figure 1. Raw material samples of corn stover and rice straw.

Table 2. Major chemical components of corn and rice straw (% dry basis).

Material Type	Chemical Components (%)			
	Cellulose	Hemicellulose	Lignin	Ash Content
Corn Stover	38.01 ± 0.41	28.04 ± 0.14	19.17 ± 0.13	3.97 ± 0.71
Rice straw	31.74 ± 0.2	21.29 ± 0.38	15.73 ± 0.33	9.12 ± 0.52

The experimental setup for UV-A pelleting was provided by Bayi Agricultural University. Figure 2 illustrates the ultrasonic-assisted molding device, which had an ultrasonic power of 500 W that could be adjusted from 20 to 100% and a hydraulic system pressure ranging from 0 to 7 MPa. The electrical energy is converted into mechanical vibration energy through the ultrasonic generator, transducer, and amplitude transformer in the molding process, resulting in a corresponding thermal effect. Consequently, the raw material under the tool undergoes absorption and conversion into heat energy, ultimately leading to the pellets due to the extrusion force provided by the hydraulic system. The diameter of the pelleting tool and aluminum mold were measured at 16 mm and 16.5 mm, respectively. Each time, approximately 1.5 g of mixed materials were loaded into the mold and compressed into pellets using a titanium tool.

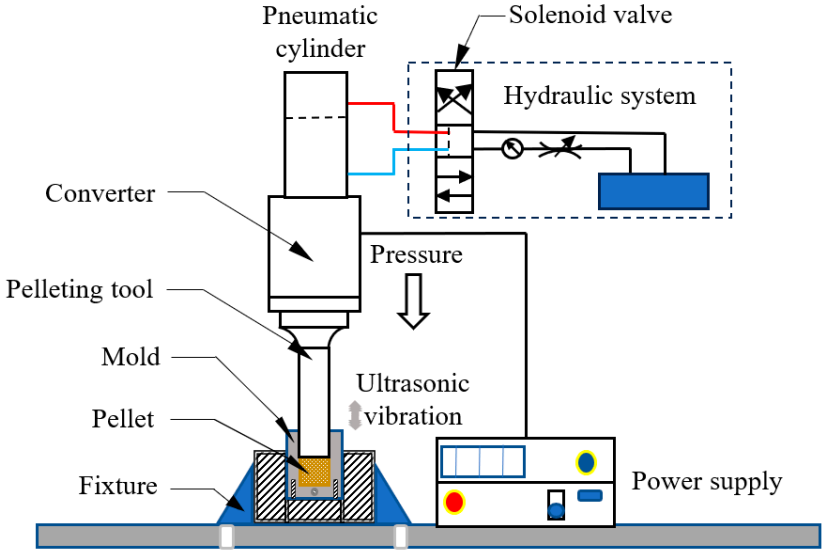

Figure 2. Ultrasonic-assisted molding device.

2.2. Experimental Design

The relative contributions of the variables and their interactions on pellet density and pellet durability were investigated through a central composite rotatable design (CCRD).

The experimental variables and their levels utilized in this study are listed in Table 3. The experimental data were analyzed using Design-Expert (version 12), and response surface graphs depicting the relationships between variables and responses were generated through RSM. To maximize pellet density and pellet durability, the optimization function in Design-Expert was employed to determine the optimal conditions [1].

Table 3. The independent variables and their corresponding levels in CCRD.

Level	Variables			
	Mixing Ratio (x_1)/%	**Molding Pressure (x_2)/MPa**	**Pelleting Time (x_3)/s**	**Ultrasonic Power (x_4)/W**
+2	50	5	50	300
+1	40	4	40	250
0	30	3	30	200
−1	20	2	20	150
−2	10	1	10	100

2.3. Pellet Density and Durability Test Methods

The density of a pellet was determined by calculating the ratio of its mass to its volume. To assess pellet durability, five pellets were weighed, and the initial weight was recorded as m_1 (g). Subsequently, they were placed in a pellet durability tester that tumbled them at a rotation speed of 50 rpm [19]. The pellets were then sieved using a No.6 U.S. sieve [20], and the weight of the retained pellets on each sieve was recorded as m_2. Pellet durability was calculated by dividing m_2 by m_1 (g) [12].

2.4. Thermogravimetric Analysis

TG and DTG were used to analyze the combustion performance of the optimized pellets. The experiments were carried out in a thermogravimetric analyzer (HTG-1, Beijing Hengjiu experimental equipment Co., Ltd., Beijing, China). After reaching the preset temperature, 10 mg pellet powder was paved uniformly in an Al_2O_3 ceramic crucible, and the sample was heated from 30 °C to 600 °C under the heating rate of 10 °C/min in an air atmosphere. The temperature was measured by a K-type thermocouple located under the crucible, and the data were recorded in real-time.

3. Results and Discussion

The experimental results obtained from RSM are presented in Table 4. Subsequently, an analysis of variance (ANOVA) was conducted to fit the experimental data to second-order polynomial models, as demonstrated in Table 5.

The models for pellet density and durability showed high significance ($p < 0.0001$), while the lack-of-fit test yielded insignificant results, indicating a good fit between the models and experimental data. The coefficient of determination (R^2) for pellet density was 0.9677. The predicted R^2 value (0.8488) is reasonably consistent with the adjusted R^2 value (0.9375). The coefficient of variation (C.V.) and Adeq Precision (AP) values acquired in this study were 0.7468% and 18.7995, respectively. The C.V. was less than 10%, and the AP was higher than 4, which suggested that the regression model for pellet density exhibited good precision in predicting the experimental results [21]. Furthermore, the comparison between the experimental data and the predicted values for density verified the reliability and accuracy of the quadratic regression model for pellet density, as depicted in Figure 3.

Table 4. The outcomes of pellet density and durability as determined by CCRD.

Run	Mixing Ratio (x_1)/%	Molding Pressure (x_2)/MPa	Pelleting Time (x_3)/s	Ultrasonic Power (x_4)/W	Pellet Density y_1/(kg/m^3)	Pellet Durability y_2/%
1	30	3	50	200	1277.97	90.06
2	20	2	20	150	1183.19	76.77
3	30	3	30	100	1220.02	79.49
4	30	3	30	300	1247.53	83.72
5	40	2	20	250	1229.65	85.50
6	20	4	40	250	1280.55	95.25
7	40	2	20	150	1208.55	81.12
8	40	2	40	250	1271.88	87.75
9	30	3	30	200	1287.96	92.67
10	40	4	20	250	1239.50	82.74
11	30	5	30	200	1284.53	95.73
12	30	3	30	200	1302.31	94.58
13	20	2	20	250	1193.27	88.89
14	30	3	30	200	1308.12	94.49
15	30	1	30	200	1215.71	85.93
16	20	4	20	150	1218.26	87.18
17	10	3	30	200	1233.99	90.69
18	30	3	10	200	1167.66	84.68
19	20	2	40	150	1261.12	84.39
20	40	4	20	150	1238.21	82.59
21	30	3	30	200	1291.04	92.33
22	30	3	30	200	1295.62	89.01
23	20	2	40	250	1276.64	93.71
24	40	4	40	150	1262.71	85.95
25	40	4	40	250	1279.55	86.35
26	30	3	30	200	1305.38	93.62
27	50	3	30	200	1266.98	82.07
28	20	4	20	250	1244.30	95.89
29	40	2	40	150	1253.38	85.98
30	20	4	40	150	1283.20	90.80

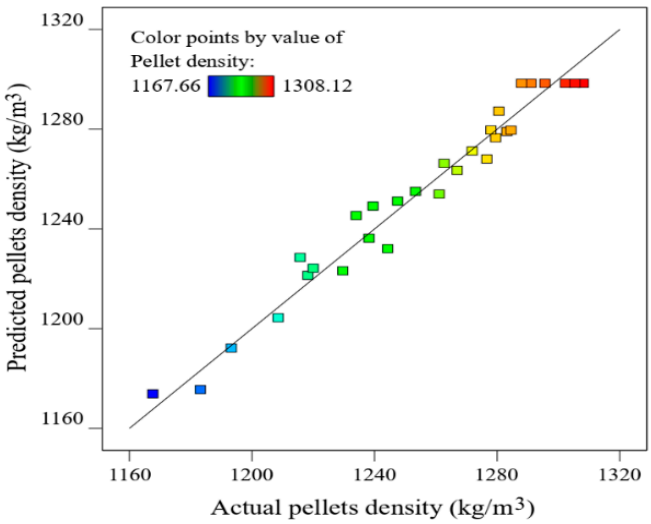

Figure 3. Comparison between the actual density and the predicted values.

Table 5. ANOVA and coefficients of the pellet density and durability in the full model.

Source	df	Pellet Density			Pellet Durability		
		Sum of Squares	*p*-Value	Coefficients	Sum of Squares	*p*-Value	Coefficients
Model	14	39,395.48	<0.0001 **	1298.41	738.34	<0.0001 **	92.78
x_1	1	493.93	0.0315 *	4.54	113.27	<0.0001 **	−2.17
x_2	1	3908.18	<0.0001 **	12.76	74.33	0.0003 **	1.76
x_3	1	16,786.33	<0.0001 **	26.45	67.53	0.0004 **	1.68
x_4	1	1089.75	0.0031 **	6.74	103.17	0.0001 **	2.07
x_1x_2	1	193.02	0.1587	−3.47	49.28	0.0016 **	−1.75
x_1x_3	1	768.40	0.0097 **	−6.93	0.1127	0.8566	−0.0839
x_1x_4	1	4.77	0.8188	0.5459	48.65	0.0017 **	−1.74
x_2x_3	1	426.53	0.0435 *	−5.16	5.76	0.2087	−0.5998
x_2x_4	1	35.02	0.5370	−1.48	12.04	0.0769	−0.8675
x_3x_4	1	6.63	0.7872	−0.6435	5.55	0.2167	−0.5889
x_1^2	1	3311.81	<0.0001 **	−10.99	64.78	0.0005 **	−1.54
x_2^2	1	3367.57	<0.0001 **	−11.08	4.94	0.2423	−0.4246
x_3^2	1	8794.22	<0.0001 **	−17.91	45.60	0.0022 **	−1.29
x_4^2	1	6308.41	<0.0001 **	−15.17	204.51	<0.0001 **	−2.73
Residual	15	1316.09	--	--	50.05		--
Lack of Fit	10	986.60	0.3433	--	28.75	0.7212	--
Pure Error	5	329.49	--	--	21.29	--	--
Cor Total	29	40,711.57	--	--	788.39	--	--

Note: The symbol "**" denotes high statistical significance ($p \leq 0.01$), while "*" indicates statistical significance ($p < 0.05$).

ANOVA analysis presented in Table 3 indicated that molding pressure, pelleting time, ultrasonic power, and the interaction of pelleting time and mixing ratio had extremely significant effects on pellet density at the statistical level of $p < 0.01$. The mixing ratio, the interaction of molding pressure, and pelleting time had a significant effect at the statistical level of $p < 0.05$. After eliminating the items with *p*-values exceeding 0.05, Equation (1) was derived to represent the response surface model for pellet density.

$$y_1 = 378.77 + 9.95x_1 + 111.07x_2 + 12.27x_3 + 2.66x_4 - 0.069x_1x_3 - 0.52x_2x_3 - 0.11x_1^2 - 11.08x_2^2 - 0.18x_3^2 - 0.0061x_4^2 \quad (1)$$

A similar method was used to analyze pellet durability. The ANOVA indicated that the values of R^2 and Adj-R^2 for pellet durability were 0.9365 and 0.8773, respectively. Meanwhile, the values of C.V. and AP obtained herein were 2.08% and 14.1665, respectively. The accuracy of the model was further validated by conducting a comparison between the experimental data and the predicted values for pellet durability, as depicted in Figure 4. The uniform points distributed around the diagonal line verified a reasonable prediction for pellet durability. All parameters, including the interaction between mixing ratio and molding pressure and mixing ratio and ultrasonic power, had a significant impact on pellet durability. After eliminating the items that were not statistically significant, Equation (2) was derived to represent the response surface model for pellet durability.

$$y_2 = -52.60 + 1.95x_1 + 14.84x_2 + 1.38x_3 + 0.670x_4 - 0.18x_1x_2 - 0.0035x_1x_4 - 0.015x_1^2 - 0.013x_3^2 - 0.0011x_4^2 \quad (2)$$

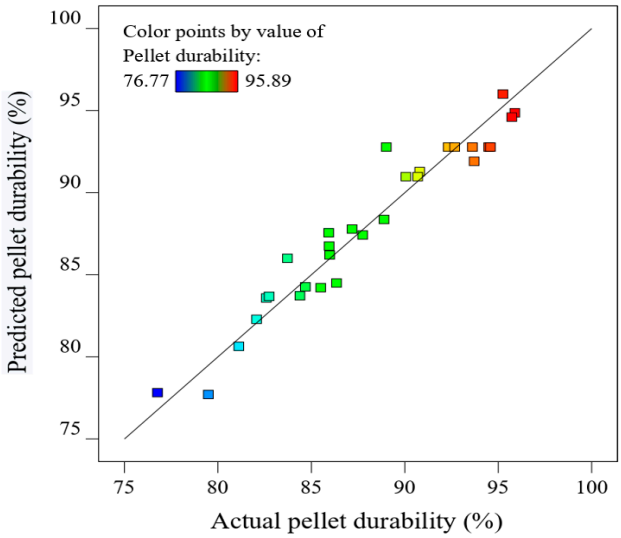

Figure 4. Comparison between experimental data and the predicted values of durability.

3.1. Interaction Effects on Pellet Density

The interaction effects of pelleting time and mixing ratio, as well as pelleting time and molding pressure on pellet density, were analyzed, as illustrated in Figure 5. Figure 5a was obtained at a molding pressure of 3 MPa and ultrasonic power of 200 W. At a mixing ratio of 10%, the pellet density increased from 1093.42 kg/m^3 to 1254.43 kg/m^3 with an increase in pelleting time. However, the maximum value of pellet density was achieved at around 41 s, reaching up to 1268.96 kg/m^3, then slightly decreasing thereafter. A similar trend was observed for a mixing ratio of 50%, where the maximum value reached was 1266.88 kg/m^3 at around 33 s. The phenomenon could be explained by requiring a certain amount of pelleting time for ultrasonic power to generate more heat that softened lignin, promoting tight binding between particles [22,23] and eliminating elastic recovery. However, longer pelleting times resulted in decreased pellet densities due to excessive heat, causing raw material volatiles to evaporate or even carbonize inside pellets [24]. As the mixing ratio increased, the initial slight increase in pellet density occurred because rice straw had greater thermal conductivity than corn stover; thus, it facilitated heat transfer that softened lignin and increased density within lower pelleting times. However, due to significant decreases in lignin content for higher levels of mixing ratios, the attraction forces between solid particles weakened and springback increased, resulting in decreased pellet densities. Pelletizing time had more significant effects on pellet density at a smaller mixing ratio.

In Figure 5b, the pellet density increased from 1084.31 kg/m^3 to 1247.44 kg/m^3 at a mixing ratio of 30% and ultrasonic power of 200 W but then decreased to 1230.76 kg/m^3 with longer pelleting time at the lower level of molding pressure. However, there was only a slight decrease after reaching the maximum value of 1283.74 kg/m^3 at the high level of molding pressure as the pelleting time increased. This could be attributed to the fact that longer pelleting time generated more heat through ultrasonic power, which softened lignin and improved pellet quality. With increasing molding pressure, the pellet density rose from 1084.31 kg/m^3 to 1176.56 kg/m^3 at shorter pelleting times, indicating that higher pressure led to significant changes in particle size and reduced porosity levels. Nevertheless, when the pressure reached around 3 MPa, the pellet density peaked at 1280.14 kg/m^3 for longer pelleting times before slightly decreasing again due to excessive heat generation by ultrasonic power, causing evaporation of moisture and organic matter in the feedstock. Previous research also reported that the temperature in the pellet increased with the increase in pelleting time and ultrasonic power [19].

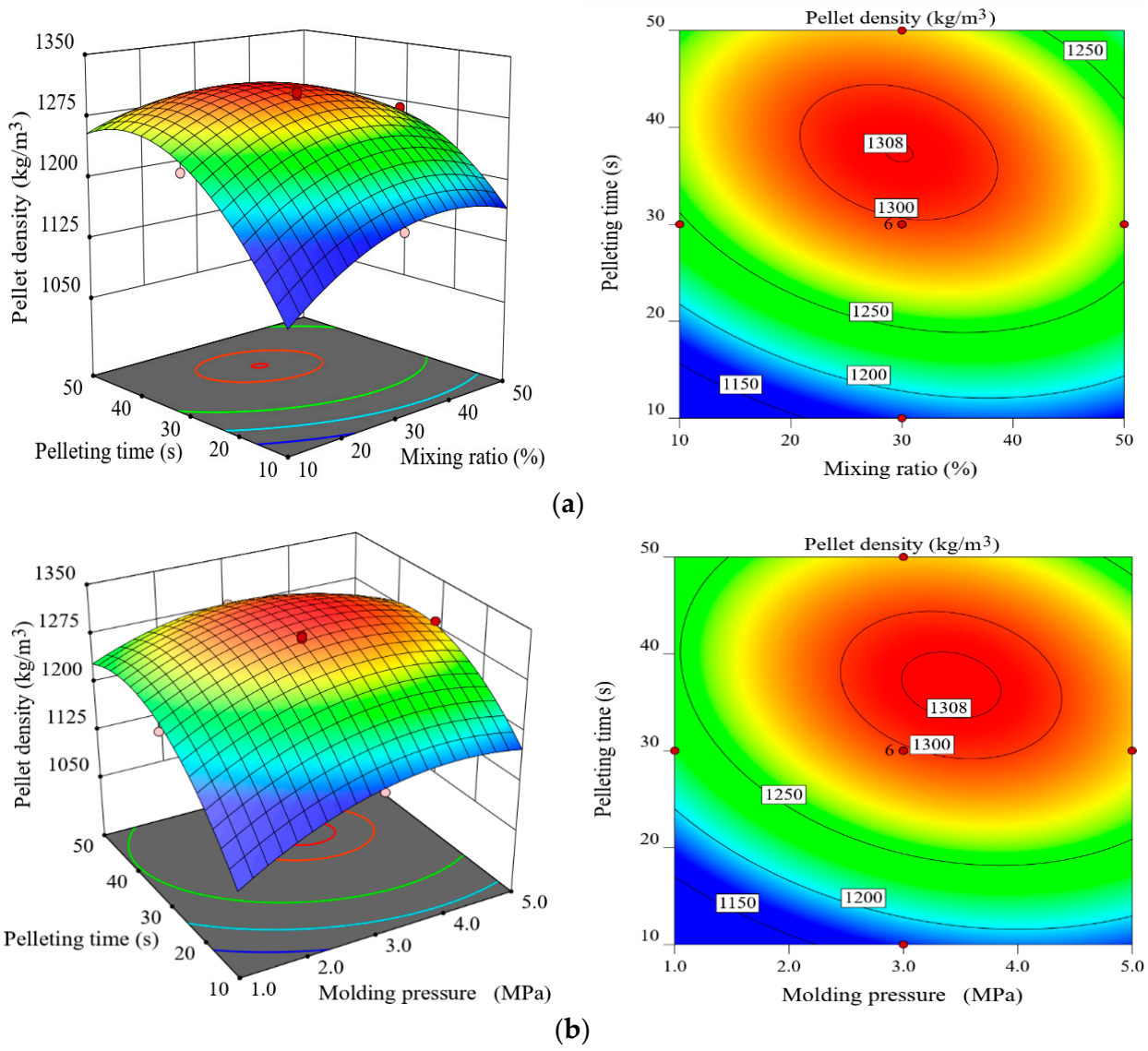

Figure 5. Response surface plots illustrating the relationship between variables and pellet density. (**a**) Pelleting time and mixing ratio; (**b**) Pelleting time and molding pressure.

3.2. Interaction Effects on Pellet Durability

Figure 6 illustrates the interaction effect of variables on pellet durability. Figure 6a was obtained by setting pelleting time and ultrasonic power at 30 s and 200 W, respectively. Pellet durability increased as molding pressure increased across all levels of the mixing ratio. This can be attributed to particles being compressed against each other, extending into surrounding crevices, thereby forming mechanical interlocks and chimerism due to increasing molding pressure. Simultaneously, stronger intermolecular forces were generated as particle spacing decreased [25]. Consequently, some brittle particles were crushed and broken down while the cell structure of biomass was disrupted, leading to the release of natural binder components such as lignin, hemicellulose, protein, and starch, which enhanced pellet durability [26]. At a mixing ratio of 10%, pellet durability improved from 78.85% to 99.82%. The impact of molding pressure on pellet durability was more pronounced at a lower mixing ratio. As the mixing ratio increased, the trend in pellet durability resembled that of pellet density under low-pressure conditions but gradually decreased under high-pressure conditions. This phenomenon could be explained by a higher mixing ratio resulting in lower lignin content and reduced particle-to-particle bonding strength.

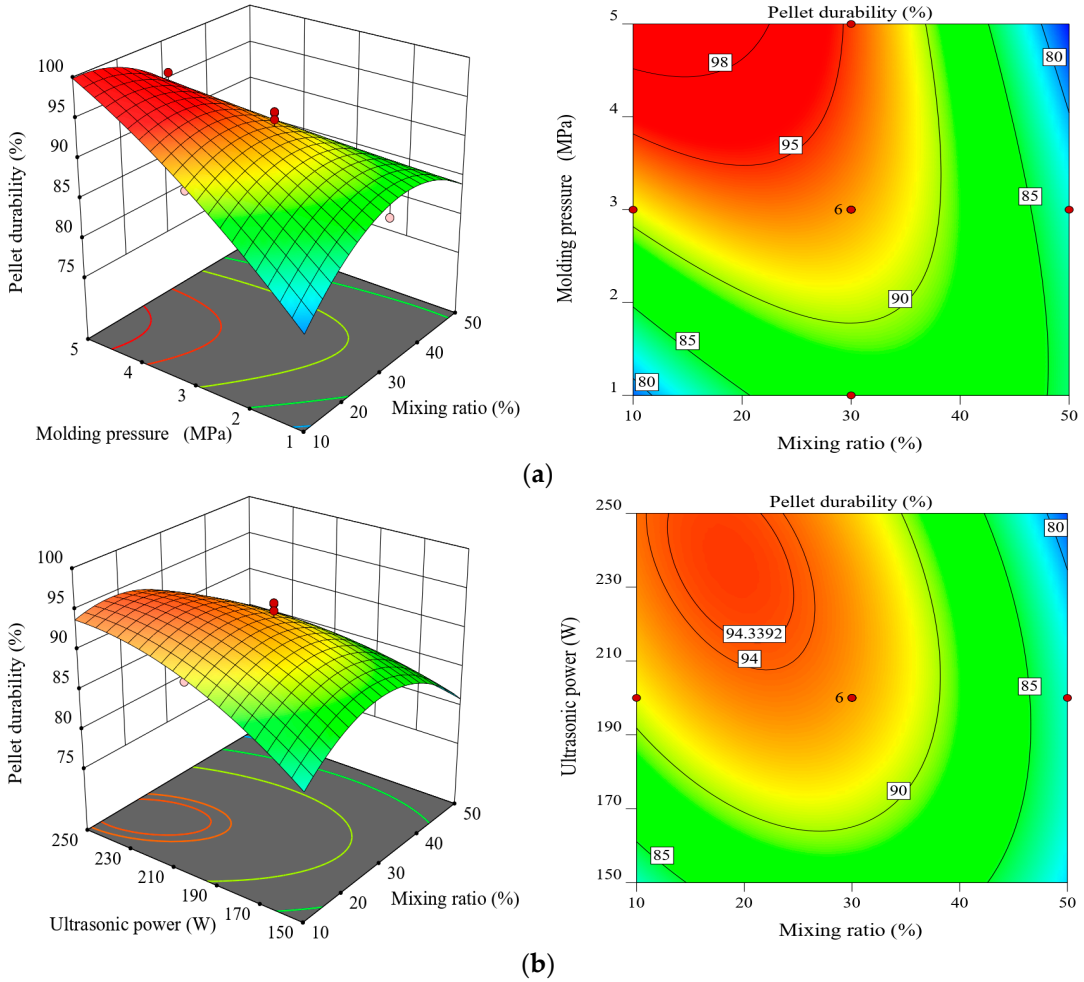

Figure 6. Response surface plots illustrating the relationship between variables and pellet durability. (**a**) Molding pressure and mixing ratio; (**b**) Ultrasonic power and mixing ratio.

Figure 6b was obtained with pelleting time and molding pressure at 30 s and 3 MPa. When the mixing ratio was set at 10%, there was an increase in pellet durability from 83.83% to 93.84% with an increase in ultrasonic power. However, after reaching its maximum value (82.57%) at 188 W, there was a slight decrease to 78.32% when the mixing ratio reached 50%. Higher ultrasonic powers generated more heat, facilitating the softening of lignin and hemicellulose to enhance particle binding at a mixing ratio of 10%. However, when the mixing ratio was 50%, there was insufficient natural adhesive to achieve this effect. Pellet durability decreased from 93.84% to 78.32% at an ultrasonic power of 250 W. It was inferred that the reason was the same as pellet density. Higher ultrasonic power may result in charring inside pellets. Li et al. [27] reported that the pellet charring ratio was up to 70% when the temperature increased to 350 °C, which was generated by ultrasonic vibration in UV-A pelleting. The effect of ultrasonic power on pellet durability was more pronounced at lower mixing ratios, while the influence of mixing ratio was more significant at higher ultrasonic powers.

3.3. Optimization and Model Verification

To obtain the optimal parameters for maximizing the pellet density and durability, the optimization function in design-expert 12 software was used, and optimized data were according to Equation (3) as the boundary conditions.

$$\begin{cases} Max(y_1, y_2) \\ s.t. \begin{cases} 10 \le x_1 \le 50 \\ 1 \le x_2 \le 5 \\ 10 \le x_3 \le 50 \\ 100 \le x_4 \le 300 \end{cases} \end{cases} \quad (3)$$

Through multi-objective optimization solution, the theoretical pellet density and durability were 1307.39 kg/m^3 and 95.89% when the optimal conditions were mixing ratio at 24.63%, molding pressure at 3.75 MPa, pelleting time at 36.65 s, and ultrasonic power at 212.20 W, respectively. The simulation results were further validated through additional confirmation experiments to compare the outcomes of the model under the condition of mixing ratio of 25%, molding pressure of 4 MPa, pelleting time of 37 s, and ultrasonic power of 200 W. The density and durability were 1301.18 kg/m^3 and 94.26%, respectively, which was closely aligned with predicted values, and the desirability was calculated as 0.997, indicating an exceptional level of agreement between the model predictions and experimental data as presented in Table 6. The pellets produced in the confirmation experiments are shown in Figure 7.

Table 6. The results from the confirmation experiment under optimal conditions.

Comparison	Process Variables				Pellet Density (kg/m^3)	Pellet Durability (%)
	Mixing Ratio/%	Molding Pressure/MPa	Pelleting Time/s	Ultrasonic Power/W		
Predicted value	24.63	3.75	36.65	212.20	1307.39	95.89
Experimental value	25	4	37	200	1301.18	94.76
Error (%)	--	--	--	--	0.47	1.18

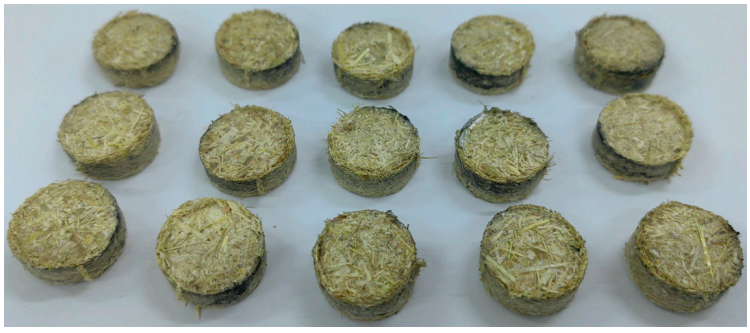

Figure 7. Pellets made from mixing material in confirmation experiments.

3.4. TG/DTG r Analysis

Figure 8 presents the weight loss and derivative weight loss curves for the optimized pellets. According to TG and DTG curves, the drying stage (I) was between 30 °C and 200 °C, where water escaped from the pellets, and the weight loss rate was within 6.67%. The volatilizing combustion stage (II) was between 200 °C and 370 °C, which was mainly due to the degradation and oxidation of cellulose and hemicellulose, as well as a few lignin. Hemicellulose and other low molecular mass substances of biomass decomposed from 200 to 270 °C, which is basically the same as the oxidative pyrolysis of hemicellulose at 160–240 °C [28]. During the rapid pyrolysis of cellulose at 270–370 °C, the DTG curve

peaked at 320 °C, and the weight loss rate was 41.01%, which may be due to the generation of a large amount of gas and less carbon. Previous research had also reported that the oxidative pyrolysis of cellulose occurred at 240–360 °C [29]. With the further increase of pellet temperature from 370 to 570 °C (III), the thermal decomposition rate of cellulose decreased rapidly, and the surface of lignin started to fire at a slower rate due to high-temperature carbonization and oxidation. This stage was dominated by lignin decomposition and coke combustion, which are difficult to pyrolytic. After 570 °C, it was the burnout stage (IV). After the combustion, the inner material of the pellet was basically burned out, and the TG and DTG curves remained stable and no longer changed.

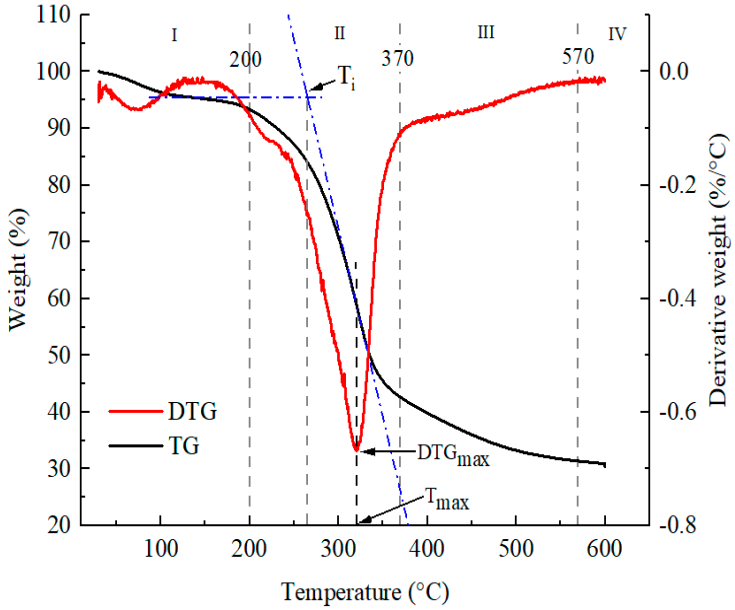

Figure 8. Weight loss and derivative weight loss curves for the optimized pellets.

DTG_{max} is the maximum weight loss rate, also known as the maximum combustion rate, which reflects the intensity of sample combustion and is the temperature/time point at which the mass change rate of the whole curve is the largest. The DTG_{max} was 0.6659%/°C, and the corresponding peak temperature T_{max} was 320 °C. Ignition temperature Ti refers to the lowest temperature of continuous combustion when the sample is heated in the experimental atmosphere, reflecting the difficulty of the sample ignition; usually, the higher the Ti, the more difficult it is to fire. Ti is generally obtained by the tangential method. Tangent as an app in origin (2021) is used to tangent the TG numerical point corresponding to the Tmax, and the baseline of the TG curve of the sample after complete dehydration is also made. The intersection point of the two lines is the ignition temperature corresponding to the sample [30]. The ignition temperature was 266 °C. The temperature at the end of combustion was burnout temperature Th, which was the temperature point at which the basic reaction of the sample was complete. It directly reflected the burnout performance of the pellet and corresponded to the temperature when the TG curve was basically unchanged or DTG approached 0%/°C. The Th in this study was 570 °C.

4. Conclusions

In this study, the CCRD was employed to ascertain the optimal conditions for pellet density and durability using rice straw and corn stover as raw materials in UV-A pelleting. Then, the combustion of the optimized pellet was analyzed with TG and DTG. The major conclusions of this study are as follows:

(1) Mathematical regression models were established, and the R^2 values for the regression models were 0.97 for pellet density and 0.94 for pellet durability, accurately predicting these properties under optimal conditions.

(2) Based on *p*-values, pelleting time, molding pressure, ultrasonic power, and mixing ratio had significant effects on pellet density. Mixing ratio, ultrasonic power, molding pressure, and pelleting time significantly influenced pellet durability. The interaction effects between mixing ratio and pelleting time, as well as molding pressure and pelleting time, were statistically significant for pellet density. Meanwhile, the interaction effects between the mixing ratio and molding pressure, as well as the mixing ratio and ultrasonic power, had an extremely significant impact on pellet durability.
(3) The optimal conditions obtained were a mixing ratio of 25%, molding pressure of 4 MPa, pelting time of 37 s, and ultrasonic power of 200 W.
(4) The combustion of the optimized pellet was divided into four stages, including the drying stage, volatilizing combustion stage, lignin decomposition, coke combustion stage, and burnout stage. The maximum weight loss rate was 0.6659%/°C, with the corresponding temperature of 320 °C. Ignition temperature and burnout temperature were 266 °C and 570 °C, respectively.

Author Contributions: Conceptualization, W.L.; methodology, W.L. and R.Y.; validation, R.Y.; writing—original draft preparation, W.L.; writing—review and editing, W.L. and L.L.; supervision, W.L.; project administration, L.L. and H.S.; funding acquisition, L.L. and H.S. All authors have read and agreed to the published version of the manuscript.

Funding: The present study was financially supported by the Natural Science Talent Support Plan of Heilongjiang Bayi Agricultural University (Grant No. ZRCPY202010), the Technological Project of Heilongjiang Province "the open competition mechanism to select the best candidates" (Grant No. 2022ZXJ05C02), and Natural Science Foundation of Heilongjiang Province (LH2021E005).

Data Availability Statement: The authors confirm that the data substantiating the conclusions of this study are accessible within the article.

Conflicts of Interest: Author Hongying Shi was employed by the Heilongjiang Boneng Ecological Environmental Protection Co., Ltd. The remaining authors declare that the research was conducted in the absence of any commercial or financial relationships that could be construed as a potential conflict of interest.

References

1. Liu, Q.; Yi, Y.; Xu, W.; Zhang, Y. Research progress of fueling utilization technology of corn straw. *J. Wuhan Polytech. Univ.* **2022**, *41*, 9–15.
2. Huo, L.; Zhao, L.; Meng, H.; Yao, Z. Study on straw multi-use potential in China. *Trans. Chin. Soc. Agric. Eng.* **2019**, *35*, 218–224.
3. Cong, H.; Meng, H.; Yu, J.; Yao, Z.; Feng, J.; Zhao, L. Analysis of long-term mechanism for development of straw industry in northeast China under guidance of "Green-concept". *Trans. Chin. Soc. Agric. Eng.* **2021**, *37*, 314–321.
4. Shinde, R.; Shahi, D.K.; Mahapatra, P.; Singh, C.S.; Naik, S.K.; Thombare, N.; Singh, A.K. Management of crop residues with special reference to the on-farm utilization methods: A review. *Ind. Crops Prod.* **2022**, *181*, 114772. [CrossRef]
5. Saleem, M. Possibility of utilizing agriculture biomass as a renewable and sustainable future energy source. *Heliyon* **2022**, *8*, e08905. [CrossRef] [PubMed]
6. Li, W.; Wang, M.; Meng, F.; Zhang, Y.; Zhang, B. A Review on the Effects of Pretreatment and Process Parameters on Properties of Pellets. *Energies* **2022**, *15*, 7303. [CrossRef]
7. Styks, J.; Wróbel, M.; Frączek, J.; Knapczyk, A. Effect of Compaction Pressure and Moisture Content on Quality Parameters of Perennial Biomass Pellets. *Energies* **2020**, *13*, 1859. [CrossRef]
8. Siyal, A.A.; Liu, Y.; Ali, B.; Mao, X.; Hussain, S.; Fu, J.; Ao, W.; Zhou, C.; Wang, L.; Liu, G.; et al. Pyrolysis of pellets prepared from pure and blended biomass feedstocks: Characterization and analysis of pellets quality. *J. Anal. Appl. Pyrolysis* **2022**, *161*, 105422. [CrossRef]
9. Zhang, Q.; Zhang, P.; Pei, Z.; Wang, D. Investigation on characteristics of corn stover and sorghum stalk processed by ultrasonic vibration-assisted pelleting. *Renew. Energy* **2017**, *101*, 1075–1086. [CrossRef]
10. Yao, Z.; Zhang, Y.; Zhao, L.; Guo, Z.; Meng, H.; Cong, H.; Cong, H. Design and experiment of biomass briquetting machine with vertical double circular mould. *Trans. Chin. Soc. Agric. Eng.* **2016**, *32*, 8–12.
11. Nasrin, A.B.; Ma, A.N.; Choo, Y.M.; Mohamad, S.; Rohaya, M.H.; Azali, A.; Zainal, Z. Oil Palm Biomass As Potential Substitution Raw Materials For Commercial Biomass Briquettes Production. *Am. J. Appl. Sci.* **2008**, *5*, 179–183. [CrossRef]
12. Li, W.; Sui, J.; Wang, L.; Song, J. The Effect of Urea Pretreatment Combined with Ultrasonic Vibration-Assisted Pelleting on Pellet Solid Density and Durability. *Processes* **2023**, *11*, 2170. [CrossRef]

13. Zhang, P.; Deines, T.D.; Pei, Z.J.; Wang, D. Ultrasonic Vibration-Assisted Pelleting of Biomass a Designed Experimental Investigation on Pellet Quality and Sugar Yield. In Proceedings of the 2010 International Manufacturing Science and Engineering Conference, Erie, PA, USA, 12–15 October 2010; pp. 1–9.
14. Zhang, P.; Pei, Z.J.; Wang, D.; Wu, X.R.; Cong, W.; Zhang, M.; Deines, T. Ultrasonic Vibration-Assisted Pelleting of Cellulosic Biomass for Biofuel Manufacturing. *J. Manuf. Sci. Eng.* **2011**, *133*, 011012. [CrossRef]
15. Zhang, P.; Zhang, Q.; Deines, T.W.; Pei, Z.; Wang, D. Ultrasonic Vibration-Assisted Peiieting of Wheat Straw: A Designed Experimentai Investigation on Pellet Quality and Sugar Yield. *J. Manuf. Sci. Eng.* **2012**, *134*, 061013. [CrossRef]
16. Fan, K.; Zhang, P.; Pei, Z.J. Ultrasonic vibration-assisted pelleting of wheat straw: A predictive model for pellet density using response surface methodology. *Biofuels* **2014**, *3*, 259–267. [CrossRef]
17. Zhang, Q.; Heng, L.; Zhang, P.; Pei, Z.J.; Wang, D.; Wilson, J.; Zhou, J. Comparison of two pelleting methods for cellulosic ethanol manufacturing: Ultrasonic vibration-assisted pelleting vs. ring-die pelleting. *Biomass Convers. Biorefinery* **2015**, *6*, 13–23. [CrossRef]
18. Zhang, Q.; Zhang, P.; Chang, S.; Pei, Z.J.; Wang, D. Optimization of Input Variables in Ultrasonic Vibration Assisted Pelleting of Cellulosic Biomass Using Multiple Response Surface Methodology. In Proceedings of the ASME 2013 International Manufacturing Science and Engineering Conference, Madison, WI, USA, 10–14 June 2013.
19. Tang, Y.; Cong, W.; Xu, J.; Zhang, P.; Liu, D. Ultrasonic vibration-assisted pelleting for cellulosic biofuels manufacturing: A study on in-pellet temperatures. *Renew. Energy* **2015**, *76*, 296–302. [CrossRef]
20. Zhang, Q.; Zhang, P.; Pei, Z.; Wang, D. Ultrasonic vibration-assisted pelleting for cellulosic biofuel manufacturing: Investigation on power consumption. *Renew. Energy* **2013**, *55*, 175–181. [CrossRef]
21. Xu, M.-X.; Zhang, P.-X.; Ji, H.-W.; Wu, Y.-C.; Liu, Z.-S.; Lu, Q. The individual and interactive effects of acid and basic oxides on ash fusibility during oxy-biomass combustion with recycled SO2. *Fuel* **2023**, *331*, 125888. [CrossRef]
22. Kaliyan, N.; Morey, R.V. Natural binders and solid bridge type binding mechanisms in briquettes and pellets made from corn stover and switchgrass. *Bioresour. Technol.* **2010**, *101*, 1082–1090. [CrossRef] [PubMed]
23. Anukam, A.; Berghel, J.; Henrikson, G.; Frodeson, S.; Ståhl, M. A review of the mechanism of bonding in densified biomass pellets. *Renew. Sustain. Energy Rev.* **2021**, *148*, 111249. [CrossRef]
24. Fan, K.Q.; Tang, Y.J.; Fang, Y. Ultrasonic Vibration-Assisted Pelleting of Cellulosic Biomass: A Review. *Adv. Mater. Res.* **2013**, *805–806*, 151–155. [CrossRef]
25. Zhang, S.; Huang, J.; Lang, S.; Zhang, X.; Chen, X.; Liang, N.; Lyu, B.; Yang, C.; Hu, N.; Wu, Y.; et al. Analysis on hot briquetting mechanism of biomass fuel pellets. *J. China Coal Soc.* **2024**, 1–15. Available online: https://link.cnki.net/urlid/11.2190.td.20240123.1056.001 (accessed on 6 April 2024).
26. Yunusa, S.U.; Mensah, E.; Preko, K.; Narra, S.; Saleh, A.; Sanfo, S. A comprehensive review on the technical aspects of biomass briquetting. *Biomass Convers. Biorefinery* **2023**. [CrossRef]
27. Li, Y.; Ning, F.; Cong, W.; Zhang, M.; Tang, Y. Investigating pellet charring and temperature in ultrasonic vibration-assisted pelleting of wheat straw for cellulosic biofuel manufacturing. *Renew. Energy* **2016**, *92*, 312–320. [CrossRef]
28. Quan, C.; Gao, N.; Song, Q. Pyrolysis of biomass components in a TGA and a fixed-bed reactor: Thermochemical behaviors, kinetics, and product characterization. *J. Anal. Appl. Pyrolysis* **2016**, *121*, 84–92. [CrossRef]
29. Xie, T.; Wei, R.; Wang, Z.; Wang, J. Comparative analysis of thermal oxidative decomposition and fire characteristics for different straw powders via thermogravimetry and cone calorimetry. *Process Saf. Environ. Prot.* **2020**, *134*, 121–130. [CrossRef]
30. Li, Y.; Peng, H.; Liao, J. Experimental Analysis of Biomass Combustion Characteristics Based on Thermogravimetric Analysis. *Guangdong Chem. Ind.* **2018**, *45*, 43–44.